PRACTICAL MODEL TO ESTIMATE DRIFT MOTION OF VESSELS BY TSUNAMI WITH CONSIDERATION OF COLLIDING WITH STRUCTURES AND STRANDING

Takashi Tomita [1] and Kazuhiko Honda [2]

Port and harbor areas are vulnerable to tsunamis, because of high population and business activities as well as low-lying areas. Furthermore many vessels, containers and cars existing in the areas may be floated and drifted by a series of tsunamis. The tsunami-drifted bodies have the potential to collide with houses and buildings and then to cause secondary damage to them. In this study, a numerical model has been developed to estimate the behavior of multiple tsunami-drifted bodies. In the present model, a drifted body due to the tsunami is moved in terms of drag and inertia forces acting on the body, which are calculated with fluid velocity distributing on side faces of the body. Furthermore, a collision model is developed and integrated with the drift model, to consider that a drifted body collides with another drift body and a fixed body. A break model of mooring system is also developed and integrated with the drift model, by which a mooring vessel can start to be drifted when the mooring system is broken. The present model is qualitatively validated through conducting simple test runs, and applied to calculations in actual bathymetry and topography.

Keywords: tsunami; floating body; drift motion; collision; numerical modeling

INTRODUCTION

A series of tsunamis cause serious damage to wide coastal areas such as inundation and destruction of houses. Furthermore in ports and harbors in which many vessels, shipping containers and cars exist, they may be floated and drifted by tsunami action. The tsunami-drifted bodies such as vessels and containers have the potential to collide with houses and structures, resulting in damaging houses and structures. Actually the 2010 Chilean earthquake tsunami pushed 680 shipping containers in the port of Talcahuano, Chile, to a town behind the port and to the sea. Parts of the containers washed on land hit and damaged residential buildings. To protect and reduce tsunami damage in ports and harbors in future, it is necessary to estimate and understand behavior of tsunami-drifted bodies as well as inundation.

To calculate a floating body and a few floating bodies under tsunami action, several numerical models have been developed. For example, Kawasaki and Hakamata (2007) developed a two-dimensional solid-gas-liquid phase flow model based on the CIP method and analyzed wave forces acting on a drifted-body in a bore-like tsunami. Yoneyama and Nagashima (2009) developed a three-dimensional model with the VOF method to calculate forces on a tsunami-drifted body. These sophisticated models can analyze the complicated fluid forces acting on a floating body and the detailed drifting behavior of a body or a few bodies. On the other hand, Ikeya et al. (2005) developed a practical method to evaluate drag and inertia forces acting on a floating body and showed validity of the method through comparison with hydraulic experiments. Since this method provides easy calculation of fluid forces acting on a floating body, it can easily apply calculation of fluid forces acting on many floating bodies.

In this study, therefore, a numerical model has been developed to estimate behavior of multiple tsunami-drifted bodies, based on the method to evaluate fluid forces by Ikeya et al. (2005). Thus, the fluid forces acting on each floating body are evaluated with drag and inertia forces in the present model. Furthermore, a new collision model is developed and integrated to consider that a floating body collides with another floating and a fixed body. A break model of a mooring system is also newly developed to allow that a moored vessel can stat to be drifted when its mooring system is broken. Fluid velocity data indispensable for evaluating the drag and inertia forces are calculated with a tsunami simulation system named STOC (Storm Surge and Tsunami Simulator in Oceans and Coastal Areas) which consists of non-hydrostatic fluid model of STOC-IC and hydrostatic quasi-3d fluid model of STOC-ML (Tomita et al. 2007, Honda and Tomita 2008). Since these fluid models can utilize air-born laser profiler data such that every house and building are identified, they can estimate the detailed

[1] Asia-Pacific Center for Coastal Disaster Research, Port and Airport Research Institute, 3-1-1 Nagase Yokosuka, 239-0826, Japan
[2] Engineering Development Division, Nagoya Research and Engineering Office for Port and Airport, Chubu Regional Bureau, Ministry of Land, Infrastructure, Transport and Tourism, 1-57-3 Higashimatabe-cho Minami-ku Nagoya, 457-0833 Japan

tsunami flow in a coastal town and therefore provide the floating process of the bodies going forward and backward on roads and hitting houses.

In this study, the present model has been developed for any types of floating bodies such as vessels, shipping containers, cars, and logs, and is applied to calculate floating process of vessels in actual bathymetry and topography. Before the application, the present model is validated qualitatively in comparison with simple test runs.

NUMERICAL MODEL TO ESTIMATE TSUNAMI-DRIFTED VESSELS

Drift Model

A drift model is developed to calculate tsunami-induced-drift behavior of hundreds floating bodies such as vessels, shipping containers, cars and other relatively large bodies. Drift motion of each floating body is driven by action of drag and inertia forces. The fluid velocity essential to evaluation of the fluid forces is calculated with fluid models of STOC-IC and STOC-ML in the state of no floating bodies. Motion modes of a floating body considered in the present model are three horizontal motions of surging, swaying and heaving, and a rotation of yawing, as shown in Fig. 1. Although vertical force driving the heaving motion is not directly calculated, the floating body can go up and down depending on the water surface elevation due to tsunami action, by keeping the height of submerged part of the body to its draft level. The shape of the floating body is a simplified rectangular solid whose length, width and height are determined in consideration of its actual length, width, height, weight and draft level.

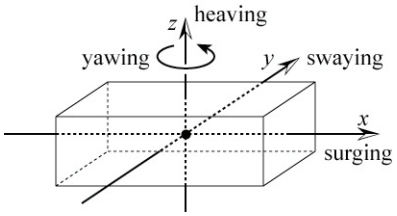

Figure 1. Motion modes considered in the drift model.

Calculation of horizontal forces in the surging and swaying directions and momentum along vertical direction uses spatial distribution of velocity on all side faces of the rectangular solid body in the same way as Ikeya et al. (2005). This method can incorporate the effect of velocity distribution with smaller scale than the floating body, which may appear around structures such as houses and buildings. The forces in the direction of surging and swaying of F_X and F_Y respectively and momentum of M_Z driving the yawing are calculated with the following equations:

$$\left.\begin{aligned} F_X &= (1-r)F_{DX1} + rF_{DX2} + F_{MX} \\ F_Y &= (1-r)F_{DY1} + rF_{DY2} + F_{MY} \\ M_Z &= (1-r)M_{DZ1} + rM_{DZ2} + M_{MZ} \end{aligned}\right\} \qquad (1)$$

$$r = \begin{cases} 1.0 - \dfrac{0.95}{0.2}\left(\dfrac{h}{D} - 1.0\right) & : \ 1 < \dfrac{h}{D} \le 1.2 \\ 0.05 & : \ 1.2 < \dfrac{h}{D} \end{cases} \qquad (2)$$

in which (X, Y, Z) is in the coordinate system determined for each floating body, B, L, and D are the width, length and draft of the simplified rectangular solid as the floating body, and h is the water depth. The first and second terms in the right hand side of Eq. 1 are the drag forces induced by vertically-changing flow and horizontally-changing flow, respectively, and the third terms are the inertia forces. r is the weight function of drag force components depending on the relative draft of h/D. Force components of Eq. 1 are as follows:

$$\left.\begin{aligned} F_{DX1} &= +\frac{\rho}{2}\iint_{sm} C_{DX1,sm}U_{sm}\left|U_{sm}\right|dYdZ+\frac{\rho}{2}\iint_{sn} C_{DX1,sn}U_{sn}\left|U_{sn}\right|dYdZ \\ F_{DY1} &= +\frac{\rho}{2}\iint_{ps} C_{DY1,ps}V_{ps}\left|V_{ps}\right|dXdZ+\frac{\rho}{2}\iint_{sb} C_{DY1,sb}V_{sb}\left|V_{sb}\right|dXdZ \\ M_{DZ1} &= -\frac{\rho}{2}\iint_{sm} C_{DX1,sm}U_{sm}\left|U_{sm}\right|YdYdZ-\frac{\rho}{2}\iint_{sn} C_{DX1,sn}U_{sn}\left|U_{sn}\right|YdYdZ \\ &\quad +\frac{\rho}{2}\iint_{ps} C_{DY1,ps}V_{ps}\left|V_{ps}\right|XdXdZ+\frac{\rho}{2}\iint_{sb} C_{DY1,sb}V_{sb}\left|V_{sb}\right|XdXdZ \end{aligned}\right\} \quad (3)$$

in which $C_{DX1,sm}$, $C_{DX1,sn}$, $C_{DY1,ps}$ and $C_{DY1,sb}$ are the drag coefficients, and U_{sm}, U_{sn} , V_{ps} and V_{sb} are the relative fluid velocities along the side faces of the floating body. The sub-suffixes of *sm*, *sn*, *ps* and *sb* indicate the values of stem, stern, portside and starboard sides of the floating body, respectively. Note that M_{DZ1} is different from the original equation in Ikeya et al. (2005), because the original M_{DZ1} provides no momentum of M_z for the floating body whose moving speed is equal to the speed of uniform flow. The other force components and drag and inertia coefficient are the same as the original.

$$\left.\begin{aligned} F_{DX2} &= \frac{\rho}{2}C_{DX2}\left(U_G^2+V_G^2\right)\frac{U_G}{\left|U_G\right|}BD \\ F_{DY2} &= \frac{\rho}{2}C_{DY2}\left(U_G^2+V_G^2\right)\frac{V_G}{\left|V_G\right|}LD \\ M_{DZ2} &= l\sqrt{F_{DX2}^2+F_{DY2}^2} \end{aligned}\right\} \quad (4)$$

in which U_G and V_G are the relative fluid velocities at the center of mass of the body, C_{DX2} and C_{DY2} are the drag coefficients in the stem-stern and portside-starboard directions, and l is the moment lever depending on the shape of the body.

$$\left.\begin{aligned} F_{MX} &= \frac{\rho}{2}C_M LD\left(\int_{sm}\frac{\partial U_{sm}}{\partial t}dY+\int_{sn}\frac{\partial U_{sn}}{\partial t}dY\right) \\ F_{MY} &= \frac{\rho}{2}C_M BD\left(\int_{ps}\frac{\partial V_{ps}}{\partial t}dX+\int_{sb}\frac{\partial V_{sb}}{\partial t}dX\right) \\ M_{MZ} &= -\frac{\rho}{2}C_M LD\left(\int_{sm}Y\frac{\partial U_{sm}}{\partial t}dY+\int_{sn}Y\frac{\partial U_{sn}}{\partial t}dY\right) \\ &\quad +\frac{\rho}{2}C_M BD\left(\int_{ps}X\frac{\partial V_{ps}}{\partial t}dX+\int_{sb}X\frac{\partial V_{sb}}{\partial t}dX\right) \end{aligned}\right\} \quad (5)$$

in which C_M is the inertia coefficient. Ikeya et al. (2005) confirmed validity of this model including the drag and inertia coefficients through comparison with experiments in steady and uniform current.

The fluid forces derived in Eq. 1 - Eq. 5 are in the coordinate system determined for each floating body. In other words, the coordinate system of a floating body is different from that of another floating body. For easy calculation therefore, coordinate transformation is mathematically conducted from the coordinate system of each floating body to that of a total calculation filed. Movement of each floating body is calculated using the following equations in terms of the fluid forces of F_x and F_y, and momentum of M_z determined in the transformed coordinate system.

$$\left.\begin{aligned} m\frac{d^2x_G}{dt^2} &= F_x \\ m\frac{d^2y_G}{dt^2} &= F_y \\ I\frac{d^2\theta_G}{dt^2} &= M_z \end{aligned}\right\} \quad (6)$$

in which (x_G, y_G) is the position of the floating body in the transformed coordinate system, θ_G is the angle of the body in a horizontal plane, m and I are the mass and inertia moment of the floating body. These equations are integrated in time to calculate drift motion of every floating body.

Collision Model

In case that many floating bodies are drifted by a tsunami, some bodies may collide with other floating bodies and fixed bodies such as a structures. A collision model is therefore developed and integrated with the drift model described in the previous section. For easy determination of a collision point at which a floating body hits with another floating and a fixed body, a contact face is set so as to cover all main parts of the floating body, as shown in Fig. 2, in which an example of a fishing boat is shown. The horizontal shape of the contact face consists of a rectangle indicated by the actual body length of L_C and width of B_C and two semicircles with the radius of R_C in the front and back of the floating body. The vertical section of the contact face is the rectangle to cover main parts which may collide with any bodies. On the other hand, the rectangular solid used to calculate motion of the floating body is usually smaller than the volume covered with the contact face. The length and width of the rectangular solid, L and B, are reduced from the actual length of L_C and B_C with a constant ratio. The ratio is determined, considering that the buoyancy calculated with the product of L, B and the draft of the body, D, is equal to the weight of the body.

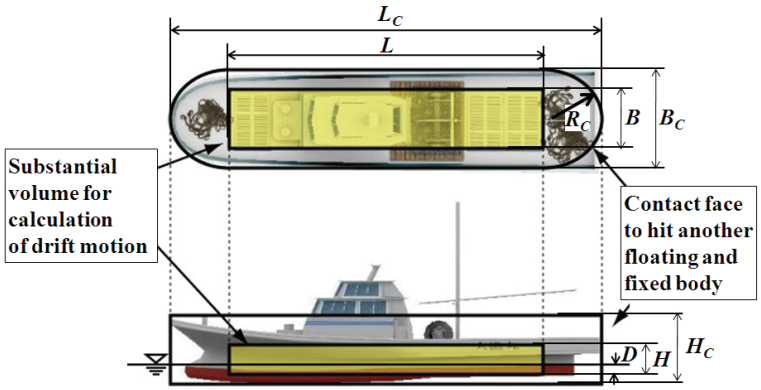

Figure 2. Contact face to determine a collision point and substantial volume for calculation of drift motion.

When a floating body (Body-B) collides with another floating (Body-A), reactive force acts on Body-B from Body-A, and drives motion of Body-B at the next time step. The direction of reactive force acting on Body-B is determined as follows. (1) Line segments of L_A and L_B are considered in the centers of both bodies colliding with each other, as shown in Fig. 3. (2) A line is set to connect both of the line segments with the shortest distance, which is the dashed line in Fig. 3. (3) The line is considered to indicate the direction of the reactive force. In the calculation including collision, part of a floating body (Body-B) may immerse the other body (Body-A) during a time step in calculation, as shown in the left figure of Fig. 3. In that case both bodies are moved parallel with the direction of reactive force until the contact faces of both bodies meets each other. To determine the location correction distances of Body-A and Body-B, the immersed distance is divided by the ratio of R_A and R_B, which are widths of contact faces for Body-A and Body-B.

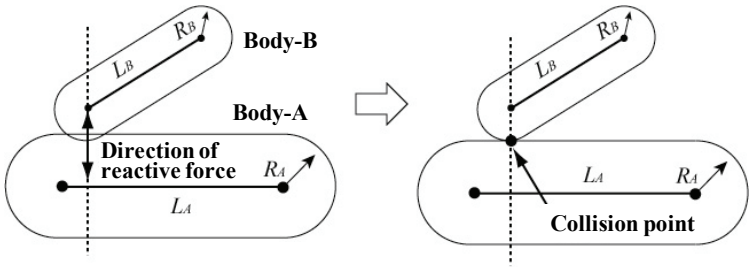

Figure 3. Direction of reactive force and position correction at the time of collision

When two floating bodies collide with each other, the momentum and angular momentum are conserved as follow:

$$\left.\begin{aligned}
m_A(u'_{GA}-u_{GA}) &= F_t e_x \\
m_A(v'_{GA}-v_{GA}) &= F_t e_y \\
m_B(u'_{GB}-u_{GB}) &= -F_t e_x \\
m_B(v'_{GB}-v_{GB}) &= -F_t e_x \\
I_A(\omega'_{GA}-\omega_{GA}) &= (x_{CA}-x_{GA})F_t e_y - (y_{CA}-y_{GA})F_t e_x \\
I_B(\omega'_{GB}-\omega_{GB}) &= -(x_{CB}-x_{GB})F_t e_y + (y_{CB}-y_{GB})F_t e_x
\end{aligned}\right\} \quad (6)$$

in which the sub-suffix of A means the values of a floating body and sub-suffix of B means those of the other floating body, m, I, (u_G, v_G), (u'_G, v'_G), ω_G, ω'_G, (x_G, y_G), and (x_C, y_C) are the mass, inertia moment, x-direction and y-direction components of moving velocity at the center of mass before collision (the values without prime) and after collision (the values with prime), angular velocity at the center of mass before collision (the value without prime) and after collision (the value with prime), location of the center of mass, and location of the collision point of each floating body. F_t is the impulse acting on each body by collision, and (e_x, e_y) is a unit vector in the direction of the impulse. An assumption that the relative velocity in the reactive force direction of each body is zero at the collision point at the time of collision yields the following equation:

$$\begin{aligned}
&\{u'_A-\omega'_A(y_{CA}-y_{GA})-u'_B+\omega'_B(y_{CB}-y_{GB})\}e_x \\
&+\{v'_A+\omega'_A(x_{CA}-x_{GA})-v'_B-\omega'_B(x_{CB}-x_{GB})\}e_y = 0
\end{aligned} \quad (7)$$

Seven equations in Eqs. 6 and 7 are used to solve seven unknown values of, (u'_{GA}, v'_{GA}), (u'_{GB}, v'_{GB}), ω'_{GA}, ω'_{GB} and F_t. A similar way is taken in case that a floating body collides with a fixed body.

In case that a floating body strands on the sea bottom and land, that is, the bottom of the contact face of the floating body meets the sea bottom and land surface, the motion of floating body is stopped. The body can be floated and moved again when the water level reached the draft level of the body.

Break Model of Mooring System

Since many vessels are moored in ports and harbors, they cannot be drifted before a tsunami breaks their mooring systems. In this study it is assumed that a vessel can start to be drifted when fluid force acting on it exceeds a certain threshold value. The threshold value depends on proof strengths of mooring ropes and mooring bitts on land. Vertical location change of the vessel due to variation of water surface elevation also creates tension force in mooring ropes and pullout and shearing forces in bitts, as shown in Fig. 4. When these forces exceed proof strengths of mooring ropes and bitts, the moored vessel are released to move depending on tsunami flow.

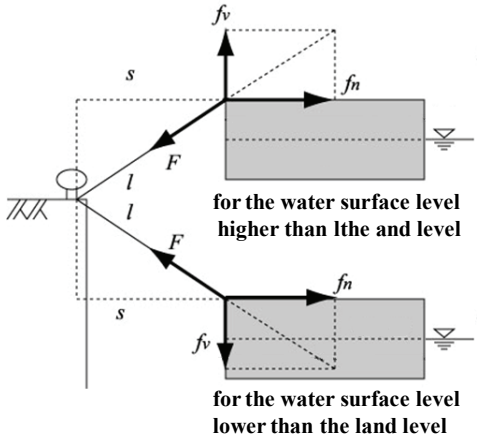

Figure 4. Breaking forces of mooring system due to water surface elevation.

TEST CALCULATIONS

Validation of the drift model integrated with the collision model is conducted in simple calculation runs. Since the drift model was basically validated by Ikeya et al. (2005), validation of the collision model is mainly checked through three test series in this study. Test series 1 include eight runs in

which a floating body is drifted in uniform flow. In the runs initial angle of the body, the partition number of the body to consider fluid velocity distribution along the body, which provides the distribution of fluid forces on the body in Eqs. 3 and 5, and the ratio of water depth and draft are changed. Although figures are omitted due to space limitation, the result in every run shows qualitatively good performance.

Test series 2 include seven runs in which a moving body in no flows collides with another moving body with various conditions of the collision point and angle and the mass ratio of two bodies. Fig. 5 indicates an example of calculation results. The length, width, draft and mass of the body A are 10 m, 2 m, 0.5 m and 10 t, respectively, and those of the body B are 15 m, 3 m, 0.444 m and 20 t. The initial speeds of the body A and body B are -0.5 m/s and 0.5 m/s respectively in the x direction. The initial angle and angular speed of the each body are 0° to the flow direction and 0 rad/s. The collision points are 1.2 m from a body edge for the body A and 0.8 m for the body B. Fig. 6 indicates the moving speed and angular speed of each body calculated with the present model. Theoretical moving speeds and angular speeds after collision are u'_A = 0.356 m/s, v'_A = -0.192 m/s and ω'_A = 0.0665 rad/s (3.81 deg/s) for the body A, and u'_B = -0.428 m/s, v'_B = 0.096 m/s, and ω'_B = 0.0222 rad/s (1.27 deg/s) for the body B. The calculated moving and angular speeds are in good agreement with the theoretical values. Moreover the good agreements are confirmed in the other runs.

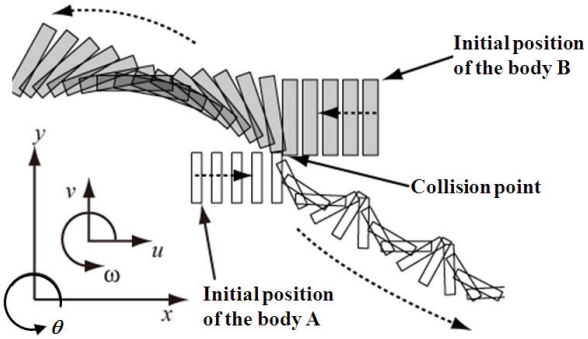

Figure 5. A test calculation of two moving bodies colliding with each other.

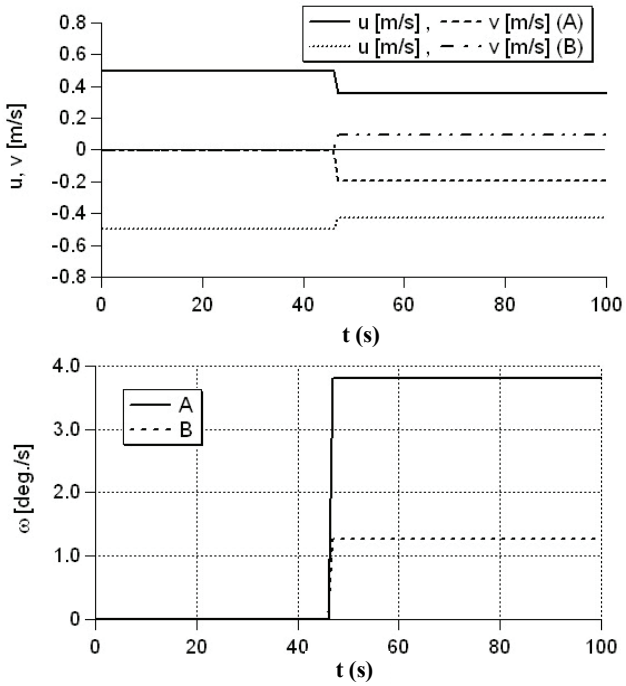

Figure 6. Moving speeds (upper) and angular speeds (lower) of the body A and B calculated with the model.

Test series 3 include six cases in which a floating body is drifted in uniform flow and collides with a fixed structure. In the runs initial angle of the body and flow speed are changed. Fig. 7 indicates a calculation result that the initial body angle is 90° to the x direction and the flow speed is u = 0.5 m/s and v = 0.5 m/s, that is, the flow direction is 45° to the x direction. Sizes of the body are 15 m in length, 3 m in width and 45 t in weight, and the draft of the body is 1 m. The body positions every 30 minutes are shown in the figure. The moving and angular speeds of the body are shownn in Fig. 8. From initiation of drift motion to collision with the fixed structure at the time of 350 s, flow action produces rotation of the body such that the long-axis direction of the body is gradually parallel to the flow direction. Moreover, the moving speed of the body is accelerated to become the flow speed until collision. When the top part of the body collides with the structure as shown in Fig. 7, reactive force from the structure causes suddenly rotation in the unticlockwise direction, and then the side of the body hits the structure again. Through this run and other five runs, it is confirmed that the drift motion of the floating body is well calculated qualitatively with the present model.

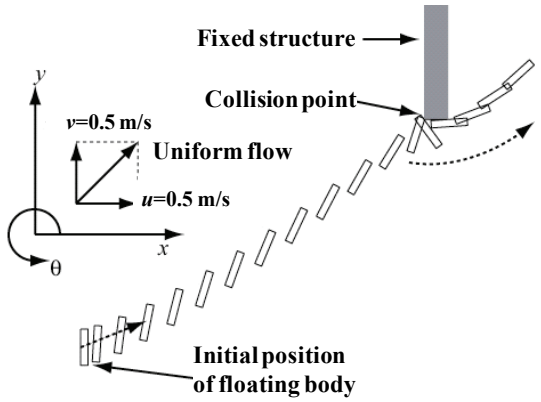

Figure 7. A test calculation of a floating body colliding with a fixed structure.

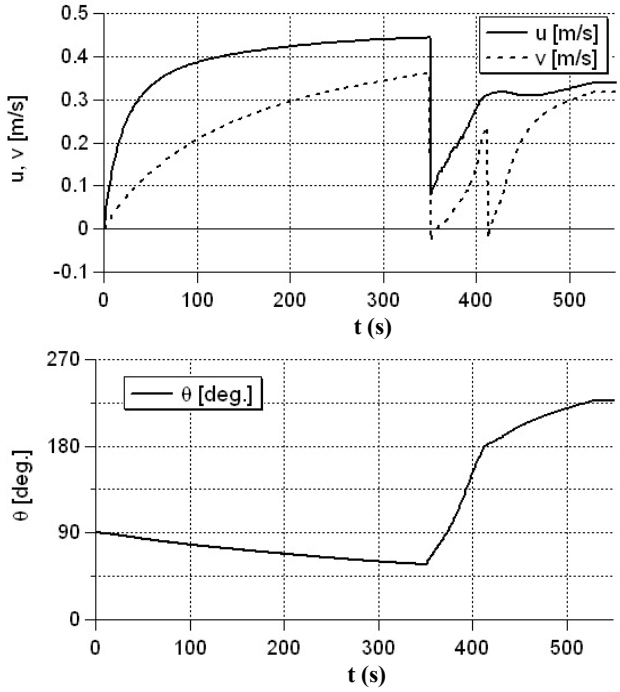

Figure 8. Moving speed components (upper) and angle (lower) of a floating body drifted in uniform flow and colliding with a structure.

APPLICATION OF STOC SYSTEM INCLUDING WITH DRIFT MODEL TO ACTUAL BATHYMETRY AND TOPOGRAPHY

Calculation of Tsunami

The STOC system (Tomita et al. 2007, Honda and Tomita 2008) is applied to calculate a tsunami in actual bathymetry and topography. To calculate the tsunami propagating from a tsunami source area and to obtain accurate results in a port area of interest, seven calculation zones are nested. The calculation grid size of the nested calculation zone is reduced by one third that of the outer calculation zone. For example, the grid size of the seventh calculation zone of the most inner zone is 2 m, and that of the sixth zone is 6 m. Fig. 9 indicates the sixth calculation zone including the seventh calculation zone which is surrounded with a thick line. In the figure there are breakwaters in a bay mouth, which is referred to as CASE 2. The other run of no breakwaters (CASE 1) is also calculated. The breakwater reduces the cross section area of the bay mouth (27,000 m^2) by 6.7 % in aperture ratio (1,800 m^2). Topographic and structure data in the seventh calculation zone is created based on air-born laser profiler data whose spatial resolution is 1 m.

The non-hydrostatic fluid model of STOC-IC with nine layers is applied in the seventh calculation zone, and the hydrostatic fluid model of STOC-ML with a single layer is applied in the other calculation zones. An incident tsunami is calculated from the tsunami source and the first tsunami wave is picked up to calculate drift motion of vessels. The tsunami height is approximately 2 m and wave period is 20 minutes at Point A in Fig. 9, as shown in Fig. 10. The time of 0 minutes in Fig. 10 means tsunami arrival at Point A.

Calculation of Drifted Vessels

Drift behavior of 158 vessels moored and landed in a rectangular area surrounded with the dashed line in Fig. 9 are calculated. Ten fishing boats among 158 vessels are landed. The number of vessels and the mooring and landing position of them are based on a field survey result on a week day. The type and size of vessels are categorized in Table 1. The threshold value to release each vessel from its moored condition is defined with the proof strengths of ropes and bitts mooring it. For calculation of drag and inertia forces acting on each vessel, fluid velocities are interpolated in 0.5 m grid spacing from the fluid velocity calculated in the condition of no vessels with the fluid models.

Furthermore, to investigate the effects of spatial resolution of velocity distribution to provide the fluid forces on vessel motions, CASE 3 and CASE 4 are conducted to calculate vessel motions in the condition of no breakwaters. In CASE 3 the interpolated fluid velocities in the 0.1 m grid spacing is constructed to calculate fluid forces on vessels from the velocity calculated with STOC-IC and STOC-ML. In CASE 4 the fluid velocity at the center of mass of each vessel is representatively used to evaluate the fluid forces. Note that the tsunami fluid velocity and water surface elevation data in the 6 m grid spacing are utilized to provide the fluid velocity distribution used for calculations of vessel motion in CASE 3 and CASE 4.

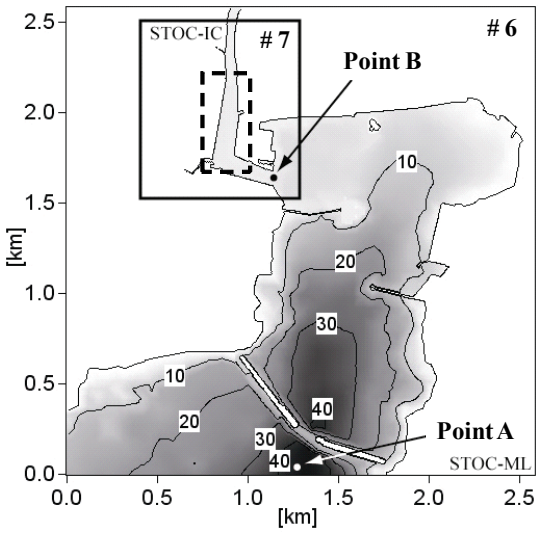

Figure 9. Bathymetry and topography of CASE 2.

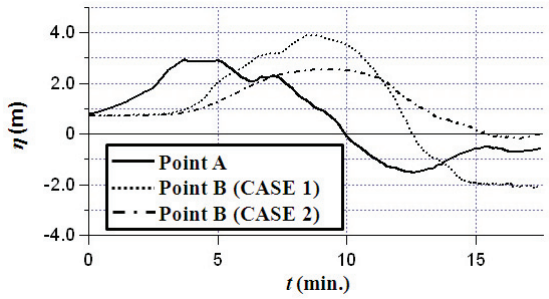

Figure 10. Time variation of water surface elevation on the mean water level (T.P.) by the tsunami.

Table 1. Type and size of vessels.

Type		Length (m)	Width (m)	Draft (m)	Number
Crane barge		41.0	15.5	0.6	1
Sand carrier		29.0	8.0	0.5	3
Fishing boat	Large	21.8	4.0	0.8	5
	Middle	17.2	3.9	0.6	37
	Small	13.1	2.9	0.5	48
	Very small	8.3	2.0	0.3	64

Calculation Results

As shown in Fig. 10, in CASE 1 the maximum water surface elevation at Point B, which locates in front of the mooring water space, reaches to 4 m above the mean water level (T.P.) due to the tsunami, and 56 vessels are drifted in consequence. On the other hand, in CASE 2 the maximum water surface elevation provided by the tsunami is 2.5 m, and only 7 small boats located on the land initially are drifted. It is clear that the bay-mouth breakwaters can reduce the tsunami effects on the moored vessels as well as the tsunami height. Furthermore, in both cases it seems to be difficult that the first tsunami wave whose height is 3 m breaks mooring systems of relatively large vessels, because the large vessels are moored to strengthen bitts with thick ropes. However, if tsunami is higher, it may break the mooring systems of large vessels and more vessels can move depending on tsunami flow and run up on land due to tsunami inundation.

Fig. 11 indicates two snapshots of the visualized result of vessel motions in CASE 1. The left figure shows the initial arrangement of vessels, and the right shows the inundated area and drifted vessels in the rectangular area surrounded with a solid line in the left figure. The state indicated in the right figure occurs 10 minutes after the tsunami arrives at Point A in the bay mouth, and in other words 3 minutes after the first vessel starts to be drifted. The tsunami runs up on the land and inundates the waterfront at first after the tsunami arrives in the port area. Then, the vessels start to be drifted, when the water surface level reaches to 2 m above the initial water surface level.

In the calculation of tsunami with the fluid models, houses and buildings are considered as obstacles to the tsunami flow, and moreover they are considered as fixed structures, which vessels collide with, in the calculation of vessel drift. Therefore, drift motions of vessels are displayed clearly and sharply in movies of vessel motions. Utilization of high-resolution structure data such that roads are reproduced in the calculation field provides easy understandings of drift behavior of vessels which go up and down in the inundated roads and collide with houses.

Comparing CASE 3 and CASE 4, the numbers of drifted vessels are 59 in CASE 3 and 58 in CASE 4. The reason why the numbers are almost the same may be that the fluid velocity changes mildly in the mooring water space set in front of the straight waterfronts, resulting in no locally-large variation of fluid forces in CASE 3. However, the result of CASE 3 on the drift process of vessels after the start of drift is significantly different from that of CASE 4, as shown in Fig. 12. The displayed area is in a rectangle indicated with the dashed line in Fig. 11. The difference in the drift process may be provided by the difference of vessel's direction produced by consideration velocity distribution along the vessel to calculate the fluid forces on it. If two vessels are at almost the same position in the tsunami flow and their directions to the flow are different from each other, fluid forces on them are also different from each other, resulting in different drift process.

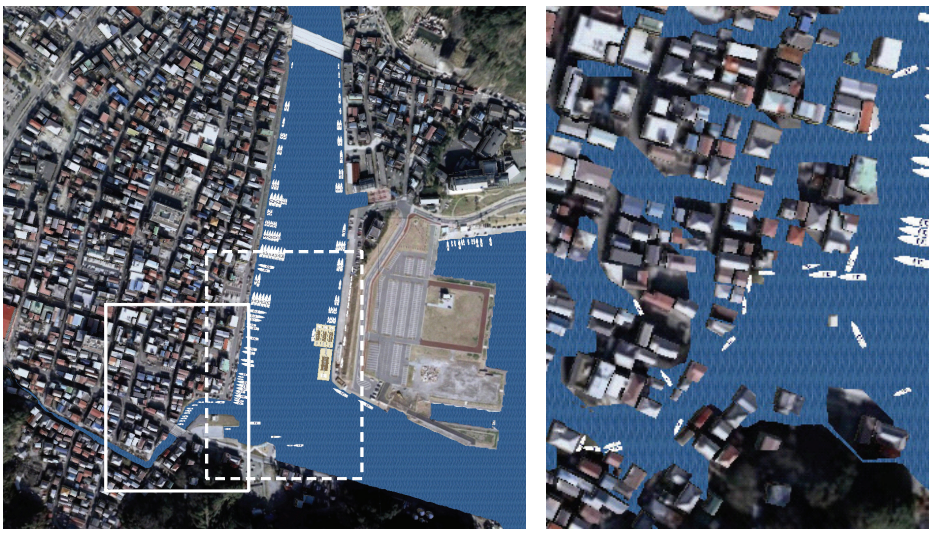

Figure 11. Initial arrangement of vessels (left) and inundation and drifted vessels (right) in the rectangular area with the solid line in the left figure 10 minutes after the tsunami arrival at Point A.

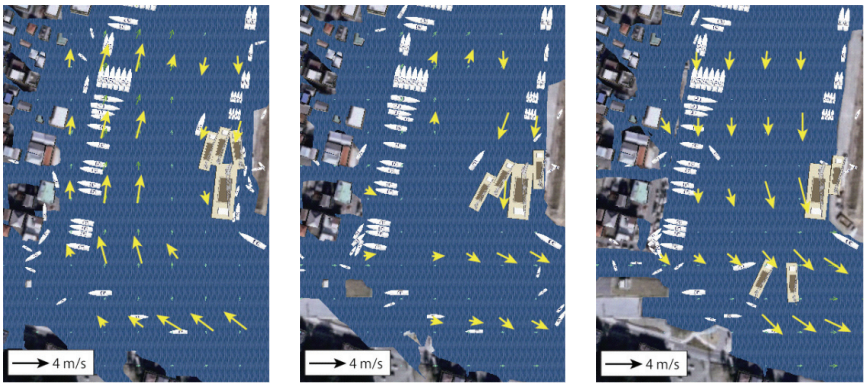

(a) CASE 3 (left: 10.5 min after tsunami arrival at Point A, middle: 12 min., right: 13.5 min.)

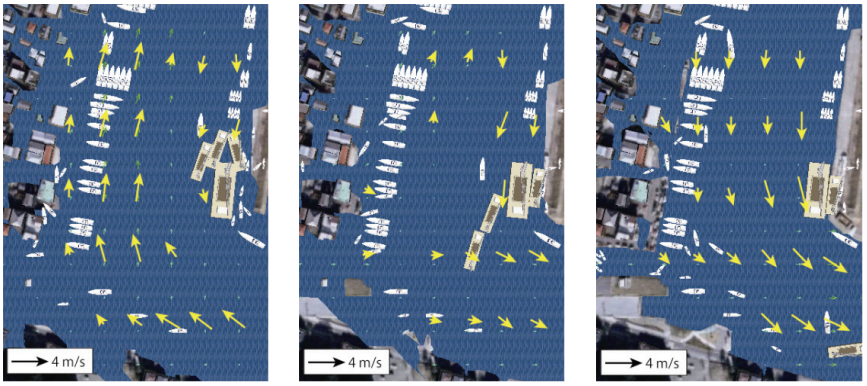

(b) CASE 4 (left: 13.5 min after tsunami arrival at Point A, middle: 15 min., right: 16.5 min.)

Figure 12. Drifted vessels and fluid velocity vectors in CASE 3 and CASE 4.

CONCLUSIONS

The numerical model is developed to calculate many tsunami-drifted bodies with consideration of collision with other floating body and fixed body and break of mooring system of a moored body. Fluid forces acting on a drifted body are drag and inertia forces calculated with fluid velocity distribution obtained a prior. The present model is validated in simple test runs, in which a floating

body is drifted in uniform flow, two moving bodies collide with each other under the condition of no flow, and a floating body in uniform flow collides with a rigid structure under various conditions. The drift model including collision with another body provides good results in all of the test runs. The drift model together with fluid models is applied to tsunami calculations in actual bathymetry and topography. Through the calculations, it is confirmed that the present model is useful to create tsunami damage image and to understand structure performance on tsunami disaster reduction, because utilization of the present model together with fluid models can estimate damage to vessels and damage to houses due to vessel's collision as well as inundation. The calculations in which houses and buildings are considered as obstacles to tsunami propagation and inundation can clearly indicate the tsunami-drifted vessels going forward and backward on roads depending on tsunami wave action. It is also shown that the vessel drift process estimated by means of the present drift model with consideration of velocity distribution along the vessel is different from the drift process based on the fluid velocity at the center of mass of the vessel. The difference may arise from vessel's direction in the tsunami flow. The drift model including the collision model and break model of mooring system should be more validated through comparison with actual tsunami damage cases and model experiments.

REFERENCES

Honda, K., and T. Tomita. 2008. Tsunami estimation including effect of coastal structures and buildings by 3d-model, *Proceedings of 31st International Conference on Coastal Engineering*, ASCE, 1433-1445.

Ikeya, T., R. Asakura, N. Fujii, M. Ohmori, T. Takeda, and K. Yanagisawa. 2005. Experiment on tsunami wave force acting on a floating body and development of an evaluation method, *Annual Journal of Coastal Engineering*, JSCE, 52, 761-765 (in Japanese).

Kawasaki, K., and M. Hakamata. 2007. Numerical analysis of time-changing wave force acting on drifting rigid structure with solid-gas-liquid phase flow model, *Proceedings of the 30th International Conference on Coastal Engineering*, ASCE, 4507-4519.

Tomita, T., K. Honda, and T. Kakinuma. 2007. Application of three-dimensional tsunami simulator to estimation of tsunami behavior around structures, *Proceedings of 30th International Conference on Coastal Engineering*, ASCE, 1677-1688.

Yoneyama, N., and H. Nagashima. 2009. Development of a three dimensional numerical analysis method for the drift behavior in tsunami, *Journal of Coastal Engineering*, JSCE, 56, 266-270 (in Japanesea).